Orbital rotation without orbital angular momentum: mechanical action of the spin part of the internal energy flow in light beams

Angelsky, O. V.; Bekshaev, A. Ya; Maksimyak, P. P.; Maksimyak, A. P.; Hanson, Steen Grüner; Zenkova, C. Yu

Published in:
Optics Express

Link to article, DOI:
10.1364/OE.20.003563

Publication date:
2012

Document Version
Publisher's PDF, also known as Version of record

Orbital rotation without orbital angular momentum: mechanical action of the spin part of the internal energy flow in light beams

O. V. Angelsky,[1,*] A. Ya. Bekshaev,[2] P. P. Maksimyak,[1] A. P. Maksimyak,[1] S. G. Hanson,[3] and C. Yu. Zenkova[4]

[1]*Correlation Optics Department, Chernivtsi National University, 2, Kotsyubinsky Str., Chernivtsi 58012, Ukraine*
[2]*Physical Department, Odessa I.I. Mechnikov National University, Dvorianska 2, Odessa 65082, Ukraine*
[3]*DTU Fotonik, Department of Photonics Engineering, DK-4000 Roskilde, Denmark*
[4]*Department of Optics and Spectroscopy, Chernivtsi National University, 2, Kotsyubinsky Str., Chernivtsi 58012, Ukraine*
[*]*angelsky@itf.cv.ua*

Abstract: The internal energy flow in a light beam can be divided into the "orbital" and "spin" parts, associated with the spatial and polarization degrees of freedom of light. In contrast to the orbital one, experimental observation of the spin flow seems problematic because it is converted into an orbital flow upon tight focusing of the beam, usually applied for energy flow detection by means of the mechanical action upon probe particles. We propose a two-beam interference technique that results in an appreciable level of spin flow in moderately focused beams and detection of the orbital motion of probe particles within a field where the transverse energy circulation is associated exclusively with the spin flow. This result can be treated as the first demonstration of mechanical action of the spin flow of a light field.

OCIS codes: (260.2160) Energy transfer; (260.5430) Polarization; (350.4855) Optical tweezers or optical manipulation; (350.4990) Particles.

References and links

1. M. J. Padgett and L. Allen, "The Poynting vector in Laguerre–Gaussian laser modes," Opt. Commun. **121**(1-3), 36–40 (1995).
2. L. Allen and M. J. Padgett, "The Poynting vector in Laguerre–Gaussian beams and the interpretation of their angular momentum density," Opt. Commun. **184**(1-4), 67–71 (2000).
3. M. V. Vasnetsov, V. N. Gorshkov, I. G. Marienko, and M. S. Soskin, "Wavefront motion in the vicinity of a phase dislocation: 'optical vortex'," Opt. Spectrosc. **88**(2), 260–265 (2000).
4. V. A. Pas'ko, M. S. Soskin, and M. V. Vasnetsov, "Transversal optical vortex," Opt. Commun. **198**(1-3), 49–56 (2001).
5. J. Lekner, "Phase and transport velocities in particle and electromagnetic beams," J. Opt. A, Pure Appl. Opt. **4**(5), 491–499 (2002).
6. J. Lekner, "Polarization of tightly focused laser beams," J. Opt. A, Pure Appl. Opt. **5**(1), 6–14 (2003).
7. H. F. Schouten, T. D. Visser, and D. Lenstra, "Optical vortices near sub-wavelength structures," J. Opt. B Quantum Semiclassical Opt. **6**(5), S404–S409 (2004).
8. A. Ya. Bekshaev and M. S. Soskin, "Rotational transformations and transverse energy flow in paraxial light beams: linear azimuthons," Opt. Lett. **31**(14), 2199–2201 (2006).
9. I. Mokhun, A. Mokhun, and J. Viktorovskaya, Singularities of the Poynting vector and the structure of optical field Proc. SPIE **6254**, 625409, 625409-10 (2006).
10. I. I. Mokhun, "Introduction to linear singular optics," in *Optical correlation techniques and applications* (Bellingham: SPIE Press PM168, 2007) pp. 1–132.
11. M. V. Berry, "Optical currents," J. Opt. A, Pure Appl. Opt. **11**(9), 094001 (2009).
12. A. Bekshaev, K. Bliokh, and M. Soskin, "Internal flows and energy circulation in light beams," J. Opt. **13**(5), 053001 (2011).
13. R. Khrobatin, I. Mokhun, and J. Viktorovskaya, "Potentiality of experimental analysis for characteristics of the Poynting vector components," Ukr. J. Phys. Opt. **9**(3), 182–186 (2008).

#159576 - $15.00 USD Received 7 Dec 2011; revised 23 Jan 2012; accepted 23 Jan 2012; published 30 Jan 2012

14. A. Ya. Bekshaev and M. S. Soskin, "Transverse energy flows in vectorial fields of paraxial beams with singularities," Opt. Commun. **271**(2), 332–348 (2007).
15. K. Y. Bliokh, M. A. Alonso, E. A. Ostrovskaya, and A. Aiello, "Angular momenta and spin-orbit interaction of nonparaxial light in free space," Phys. Rev. A **82**(6), 063825 (2010).
16. A. Ya. Bekshaev, "Spin angular momentum of inhomogeneous and transversely limited light beams," Proc. SPIE **6254**, 625407, 625407-8 (2006).
17. A. Bekshaev and M. Vasnetsov, "Vortex flow of light: 'Spin' and 'orbital' flows in a circularly polarized paraxial beam," in *Twisted Photons. Applications of Light with Orbital Angular Momentum* (Weinheim: Wiley-VCH, 2011), pp. 13–24.
18. A. Ya. Bekshaev, "Oblique section of a paraxial light beam: criteria for azimuthal energy flow and orbital angular momentum," J. Opt. A, Pure Appl. Opt. **11**(9), 094003 (2009).
19. A. Ya. Bekshaev, "Role of azimuthal energy flows in the geometric spin Hall effect of light," arXiv:1106.0982v1 [physics.optics] (6 Jun 2011).
20. K. Yu. Bliokh and Y. P. Bliokh, "Conservation of angular momentum, transverse shift, and spin Hall effect in reflection and refraction of an electromagnetic wave packet," Phys. Rev. Lett. **96**(7), 073903 (2006).
21. O. Hosten and P. Kwiat, "Observation of the spin hall effect of light via weak measurements," Science **319**(5864), 787–790 (2008).
22. A. Aiello, N. Lindlein, Ch. Marquardt, and G. Leuchs, "Transverse angular momentum and geometric spin Hall effect of light," Phys. Rev. Lett. **103**(10), 100401 (2009).
23. A. Ya. Bekshaev, "Transverse energy flow and the "running" behaviour of the instantaneous field distribution of a light beam," arXiv:1108.0784 [physics.optics] (3 Aug 2011).
24. A. T. O'Neil, I. MacVicar, L. Allen, and M. J. Padgett, "Intrinsic and extrinsic nature of the orbital angular momentum of a light beam," Phys. Rev. Lett. **88**(5), 053601 (2002).
25. V. Garces-Chavez, D. McGloin, M. D. Summers, A. Fernandez-Nieves, G. C. Spalding, G. Cristobal, and K. Dholakia, "The reconstruction of optical angular momentum after distortion in amplitude, phase and polarization," J. Opt. A, Pure Appl. Opt. **6**(5), S235–S238 (2004).
26. Y. Zhao, J. S. Edgar, G. D. M. Jeffries, D. McGloin, and D. T. Chiu, "Spin-to-orbital angular momentum conversion in a strongly focused optical beam," Phys. Rev. Lett. **99**(7), 073901 (2007).
27. M. Dienerowitz, M. Mazilu, and K. Dholakia, "Optical manipulation of nanoparticles: a review," J. Nanophoton. **2**(1), 021875 (2008).
28. A. Y. Bekshaev, O. V. Angelsky, S. V. Sviridova, and C. Yu. Zenkova, "Mechanical action of inhomogeneously polarized optical fields and detection of the internal energy flows," Adv. Opt. Technol. **2011**, 723901 (2011).
29. R. A. Beth, "Mechanical detection and measurement of the angular momentum of light," Phys. Rev. **50**(2), 115–125 (1936).
30. T. A. Nieminen, A. B. Stilgoe, N. R. Heckenberg, and H. Rubinsztein-Dunlop, "Angular momentum of a strongly focused Gaussian beam," J. Opt. A, Pure Appl. Opt. **10**(11), 115005 (2008).
31. O. V. Angelsky, N. N. Dominikov, P. P. Maksimyak, and T. Tudor, "Experimental revealing of polarization waves," Appl. Opt. **38**(14), 3112–3117 (1999).
32. O. V. Angelsky, S. B. Yermolenko, C. Yu. Zenkova, and A. O. Angelskaya, "Polarization manifestations of correlation (intrinsic coherence) of optical fields," Appl. Opt. **47**(29), 5492–5499 (2008).
33. O. V. Angelsky, M. P. Gorsky, P. P. Maksimyak, A. P. Maksimyak, S. G. Hanson, and C. Yu. Zenkova, "Investigation of optical currents in coherent and partially coherent vector fields," Opt. Express **19**(2), 660–672 (2011).
34. A. Gerrard and J. M. Burch, *Introduction to Matrix Methods in Optics* (London, Wiley-Interscience, 1975).
35. A. Ashkin, *Optical Trapping and Manipulation of Neutral Particles Using Lasers* (Singapore: Hackensack, NJ: World Scientific, 2006).
36. X.-L. Wang, J. Chen, Y. Li, J. Ding, C.-S. Guo, and H.-T. Wang, "Optical orbital angular momentum from the curl of polarization," Phys. Rev. Lett. **105**(25), 253602 (2010).
37. S. Yan, B. Yao, and M. Lei, "Comment on "optical orbital angular momentum from the curl of polarization"," Phys. Rev. Lett. **106**(18), 189301, author reply 189302 (2011).

1. Introduction

The study of internal energy flows is a rapidly developing branch of physical optics (see, e.g., Refs [1–19].). The internal flows (optical currents) not only constitute an "energy skeleton" of a light field reflecting important physical characteristics of its spatial structure. They have proven to be valuable instruments for investigation of fundamental dynamical and geometrical aspects of the light fields' evolution and transformations [1–12], providing a natural language for explaining the special features of singular fields [1–4,7–15], fields with angular momentum [8,14–18] and for interpreting the effects of spin-orbit interaction of light [12,18–22]. As physically meaningful and universal parameters of light fields, they offer disclosure of physical mechanisms of the beam transformation upon free and restricted

#159576 - $15.00 USD Received 7 Dec 2011; revised 23 Jan 2012; accepted 23 Jan 2012; published 30 Jan 2012

propagation and put forward attractive possibilities for characterization of arbitrary light fields [12].

In the usual case of a monochromatic electromagnetic field, the electric and magnetic vectors can be written as $\mathrm{Re}\left[\mathbf{E}\exp\left(-i\omega t\right)\right]$ and $\mathrm{Re}\left[\mathbf{H}\exp\left(-i\omega t\right)\right]$ with complex amplitudes $\mathbf{E}$ and $\mathbf{H}$ (ω is the radiation frequency). Subsequently, the time-average energy flow density is expressed by the Poynting vector $\mathbf{S}$ or the electromagnetic momentum density $\mathbf{p}$:

$$\mathbf{S} = c^2\mathbf{p} = gc\,\mathrm{Re}\left(\mathbf{E}^* \times \mathbf{H}\right) \tag{1}$$

($g = \left(8\pi\right)^{-1}$ in the Gaussian system of units, c is the light velocity). The total quantity [Eq. (1)] can be subdivided into the spin momentum density (SMD) and orbital momentum density (OMD), $\mathbf{p} = \mathbf{p}_S + \mathbf{p}_O$, according to which sort of beam angular momentum they are able to generate [11,14,15]:

$$p_S = \frac{g}{4\omega}\mathrm{Im}\left[\nabla \times \left(E^* \times E + H^* \times H\right)\right],\ \ p_O = \frac{g}{2\omega}\mathrm{Im}\left[E^* \cdot \left(\nabla\right)E + H^* \cdot \left(\nabla\right)H\right] \tag{2}$$

where $\mathbf{E}^* \cdot \left(\nabla\right)\mathbf{E} = E_x^*\nabla E_x + E_y^*\nabla E_y + E_z^*\nabla E_z$. The particular properties of the SMD and OMD contributions [Eq. (2)] reflect specific features of the "intrinsic" rotation associated with the spin of photons ($\mathbf{p}_S$) and of the macroscopic energy transfer ($\mathbf{p}_O$) in a light field. The quantities introduced by Eq. (2) provide deeper insight into the details of the light field evolution, and allow one to describe interrelations between the spin and orbital degrees of freedom of light [12,15–17,19–23]. However, the wide practical application of the internal flow parameters is hampered by difficulties in their experimental measurement and/or visualization. At present, only indirect procedures are available, e.g., via the Stokes polarimetry [13], where the energy flow pattern is calculated from the measured amplitude, phase and polarization data. In this context, possibilities coupled with the energy flow visualization via the motion of probe particles, suspended within an optical field, have attracted special attention [24–28]. This technique relies on the assumption that the force acting on a particle is proportional to the local value of the field momentum. Though with serious precautions [12,28], this assumption is qualitatively justified for the OMD $\mathbf{p}_O$, whereas even the physical explanation of how the spin momentum can be transferred from the field to a particle is not clear. For example, as is well established for a long time [29], a circularly polarized beam as a whole, as well as any part of its transverse cross section, carries the "pure" angular momentum that can cause spinning motion of the absorbing particle, but there is no clear understanding whether and how the translational or orbital motion can appear in this situation [12,17]. Besides, the spin flow does not manifest itself in the visible changes of the beam profile upon propagation [12,14]. Although recent calculations [28] suggest no significant differences in the mechanical action of the SMD and OMD, a direct unambiguous verification of their mechanical equivalence (e.g., in their ability to produce corresponding light pressure on material objects) is highly desirable [12,17].

In the present paper, we describe experimental observations of the polarization-dependent orbital motion of suspended probe particles in a transversely inhomogeneous beam with circular polarization where rotational action of the OMD is absent or negligible. To the best of our knowledge, these results can be considered as the first experimental evidence of the mechanical action of the spin momentum (spin energy flow) of a light beam.

#159576 - $15.00 USD Received 7 Dec 2011; revised 23 Jan 2012; accepted 23 Jan 2012; published 30 Jan 2012

2. Spin and orbital flows in paraxial beams

Let us consider a paraxial light beam propagating along the *z*-axis, and let the transverse plane be parameterized by coordinate axes *x*, *y*. The spatial distribution of the electric and magnetic vectors in this beam can be described as [12,14,17]

$$\mathbf{E} = \exp(ikz)\left(\mathbf{u} + \frac{i}{k}\mathbf{e}_z \operatorname{div}\mathbf{u}\right), \quad \mathbf{H} = \exp(ikz)\left[(\mathbf{e}_z \times \mathbf{u}) + \frac{i}{k}\mathbf{e}_z\left(\nabla_\perp \cdot (\mathbf{e}_z \times \mathbf{u})\right)\right] \quad (3)$$

where the slowly varying vector complex amplitude $\mathbf{u} = \mathbf{u}(x, y, z)$ is related to the complex amplitudes of the orthogonal polarization components of the fields [Eq. (3)], $\mathbf{e}_z$ is the unit vector in the longitudinal direction, $k = \omega/c$ is the radiation wavenumber. In the circular-polarization basis

$$\mathbf{e}_\sigma = \frac{1}{\sqrt{2}}(\mathbf{e}_x + i\sigma\mathbf{e}_y)$$

($\mathbf{e}_x$, $\mathbf{e}_y$ are unit vectors of the transverse coordinates, $\sigma = \pm 1$ is the photon spin number, or helicity),

$$\mathbf{u} = \mathbf{e}_+ u_+ + \mathbf{e}_- u_-, \quad (4)$$

$u_\sigma \equiv u_\sigma(x, y, z)$ is the scalar complex amplitude of the corresponding circularly polarized component [17] (subscripts "+" and "–" in Eq. (4) stand for $\sigma = +1$ or $\sigma = -1$). In paraxial beams, the SMD is always transverse ($\mathbf{p}_S \cdot \mathbf{e}_z = 0$) whereas the OMD consists of the longitudinal part, expressing the 'main' energy flow along the propagation direction, and the transverse part $\mathbf{p}_{O\perp}$ ($\mathbf{p}_{O\perp} \cdot \mathbf{e}_z = 0$) which describes the internal energy redistribution during the beam propagation. By using Eq. (3) and introducing 'partial' intensity and phase distributions,

$$I_\sigma(x, y, z) = cg\left|u_\sigma(x, y, z)\right|^2, \quad \varphi_\sigma = \frac{1}{2i}\ln\frac{u_\sigma}{u_\sigma^*}, \quad (5)$$

the SMD and the transverse part of the OMD [see Eq. (2)] can be expressed as sums of contributions belonging to the orthogonal polarization components,

$$\mathbf{p}_S = \mathbf{p}_{+S} + \mathbf{p}_{-S}, \quad \mathbf{p}_{O\perp} = \mathbf{p}_{+O} + \mathbf{p}_{-O}, \quad (6)$$

where [12]

$$\mathbf{p}_{\sigma S} = -\frac{\sigma}{2\omega c}\left[\mathbf{e}_z \times \nabla_\perp I_\sigma\right] = \frac{\sigma}{2\omega c}\nabla_\perp \times (\mathbf{e}_z I_\sigma), \quad (7)$$

$$\mathbf{p}_{\sigma O} = \frac{g}{\omega}\operatorname{Im}\left(u_\sigma^* \nabla_\perp u_\sigma\right) = \frac{1}{\omega c} I_\sigma \nabla_\perp \varphi_\sigma \quad (8)$$

and $\nabla_\perp = \mathbf{e}_x(\partial/\partial x) + \mathbf{e}_y(\partial/\partial y)$ is the transverse gradient.

In particular, Eq. (7) means that in beams with homogeneous circular polarization but inhomogeneous intensity, the SMD circulates around the intensity extrema [12,14,17]. In contrast, the internal OMD [Eq. (8)] is directed along the transverse phase gradient, and it is not difficult to realize conditions where the OMD vanishes or distinctly differs from the spin

#159576 - $15.00 USD Received 7 Dec 2011; revised 23 Jan 2012; accepted 23 Jan 2012; published 30 Jan 2012

contribution, e.g., in direction, so that both contributions can be easily separated in an experiment.

3. Analysis of the experimental approach

Direct observation of the internal energy flow via the field-induced motion of probe particles within a collimated laser beam is generally difficult because the transverse light pressure associated with momentum densities [Eqs. (7) and (8)] is rather weak for usual beam intensities. To enlarge the effect, in usual schemes [24–27] a cell with suspended particles is placed near the focal plane of the strongly focusing objective, in which the size of the incident beam is efficiently reduced. The high numerical aperture (NA) of the objective guarantees sufficient concentration of the light energy to provide noticeable mechanical action. However, high NA is unfavourable for the SMD investigation since tight focusing of a circularly polarized beam induces partial conversion of the initial spin flow into an orbital one [12,26] and, consequently, even if the mechanical action is observed, one cannot definitely exclude that it is caused by the conversion-generated OMD. To avoid this ambiguity, the focusing strength should not be high: in accordance with known data [30], the spin-orbital conversion is negligible (does not exceed 1%) at NA $\lesssim$ 0.2 (focusing angle $\theta \approx 11°$). Of course, this leads to certain loss in the energy concentration; however, one can avoid essential reduction of the focal-region SMD, if lowering the intensity is compensated by increasing the beam inhomogeneity [see Eq. (7)].

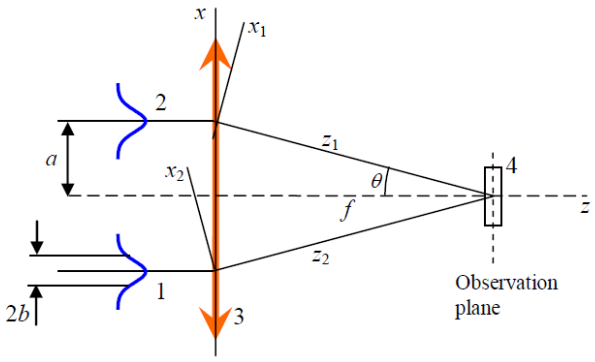

Fig. 1. Schematic of the experimental setup: (1), (2) input beams, (3) objective lens schematized by the double arrow, (4) cell with probing particles suspended in the water. Axes x_j and z_j of the involved frames (see Eqs. (10)) are shown, axes y_j are orthogonal to the figure plane.

At this point, the ideas of polarization interferometry developed in Refs [31,32]. can be employed (see Fig. 1). With this approach, the internal flows are studied in the field formed by superposition of two beams. Their polarizations (circular, elliptic, linear), phases, intensities and degree of mutual coherence can be varied within a wide range, which provides the possibility to create a diversity of optical fields with desirable properties [33]. By controlling the angle between the beams' axes and relative phase shift between the beams, one may regulate the spatial intensity modulation (interference pattern) as well as the spatial inhomogeneity of the polarization of the resulting field, independently.

In our experiments, two identical beams obtained from a semiconductor laser (λ = 0.67 μm) with radii $b = 0.7$ mm (measured at the intensity level e^{-1} of maximum) approach a micro-objective with focal distance $f = 10$ mm. The beams are parallel to the objective axis and are located at a distance $a = 1.3$ mm from it which provides the effective focusing angle $\theta = \arctan(a/f) \approx 7.4°$ and NA = 0.16; after focusing, they interfere in the focal region of the objective. If the beams are circularly polarized, they can be described by the terms in Eqs.

#159576 - $15.00 USD Received 7 Dec 2011; revised 23 Jan 2012; accepted 23 Jan 2012; published 30 Jan 2012

(4) – Eq. (8) corresponding to either $\sigma = +1$ or –1; once the helicity is fixed, the subscript σ can be omitted from subsequent equations. Let both beams be Gaussian with the nominal input (just before the lens) complex amplitude distribution

$$u_j(x,y,z) = A_0 \exp\left(-\frac{\left[x + (-1)^j a\right]^2 + y^2}{2b^2} \right) \quad (j = 1,2). \tag{9}$$

Behind the objective, each beam propagates along its own axis z_j with focusing angle ~ $\arctan(b/f) \approx 0.07$ rad, which practically corresponds to the paraxial regime. Therefore, in the proper coordinate frame (x_j, y_j, z_j) (see Fig. 1), which is connected to the laboratory frame (x, y, z) by the relations

$$x_j = \left[x + (-1)^j a\right]\cos\theta - (-1)^j z \sin\theta, \quad y_j = y, \quad z_{1,2} = (-1)^j \left[x + (-1)^j a\right]\sin\theta + z\cos\theta, \tag{10}$$

its evolution is described by the equation

$$u_j(x_j, y_j, z_j) = \eta A_0 \frac{\left(1 - \frac{z_j}{f}\right) - i\frac{z_j}{z_R}}{\left(1 - \frac{z_j}{f}\right)^2 + \left(\frac{z_j}{z_R}\right)^2} \exp\left\{ -\frac{1}{2}\left(x_j^2 + y_j^2\right) \frac{\frac{1}{b^2} - \frac{ik}{z_R}\left[\frac{z_j}{z_R} - \frac{z_R}{f}\left(1 - \frac{z_j}{f}\right)\right]}{\left(1 - \frac{z_j}{f}\right)^2 + \left(\frac{z_j}{z_R}\right)^2} \right\}, \tag{11}$$

where the coefficient η accounts for the energy losses in the focusing optical system, and $z_R = kb^2$. Eq. (11) can be readily derived from the common theory of Gaussian beams (see, e.g., Ref [34].). Then, neglecting the small (in agreement with Eq. (3)) longitudinal components, the resulting amplitude distribution in the focal region can be found from equation

$$\left[u(x,y,z)\exp(ikz)\right]_{z=f+\delta} = u_1(x_1, y, z_1)\exp(ikz_1) + u_2(x_2, y, z_2)\exp(ikz_2) \tag{12}$$

where δ specifies the exact location of the observation plane with respect to the focus (in experiment, δ was adjusted empirically to provide the best conditions for particle trapping and manipulation), z_j and x_j should be replaced by their expressions, Eq. (10), with allowance for $z = f + \delta$.

Of course, Eq. (12) is immediately applicable only to the *y*-components of the field; as for the *x*-components, it rather unites their projections onto the observation plane, proportional to cosθ (see Fig. 1), However, in the special conditions of the experiment, $\cos\theta \approx 1$ with accuracy of 1%, and the scalar relation Eq. (12) can be safely used for the whole circularly polarized field. Other projections of the *x*-components give rise to the longitudinal field component in the cell 4 of Fig. 1, which is quite noticeable (~13% of the transverse field amplitude). Nevertheless, this longitudinal component possesses no optical vortex and carries no azimuthal OMD so it can be omitted when analyzing the expected rotatory action of the focused field.

The properties of the interference pattern, calculated via Eqs. (7), (8) and (10) – (12) for conditions of Fig. 1, are illustrated in Fig. 2. It is seen that the circulatory flow of the spin nature exists within each lobe, while the OMD is, in fact, completely radial, attributed to the beam divergence. This radial field momentum can be used for probing particle confinement at a desirable off-center position [35], allowing observation of the SMD-induced orbital motion.

#159576 - $15.00 USD Received 7 Dec 2011; revised 23 Jan 2012; accepted 23 Jan 2012; published 30 Jan 2012

Within an inhomogeneous optical field, any dielectric particle is subjected to the gradient force [27] that pulls the particle towards the intensity maximum, here the beam axis; in contrast, the radial OMD of a divergent beam produces the radial light pressure that pushes the particle away from the axis. As a result, both forces can compensate each other at certain off-axial points within the central lobe of the interference pattern (e.g., points A and B in Fig. 2d), permitting stable trapping the particle at a position where azimuthal action of the SMD is the most efficient (compare Fig. 2d and Figs. 2a, 2b). In experiment, such conditions occur if the observation plane is located several microns behind the focus ($\delta > 0$).

Figure 2c shows that due to strong intensity modulation, the SMD in the two-beam interference pattern is approximately 2.5 times higher than in a single Gaussian beam focused with the same NA objective. Noticeably, to reach the equivalent SMD level in a single Gaussian beam, conditions with NA ≈0.4 should be realized when more than 10% of the initial SMD would be transformed to the OMD [30]. The interference technique of the focal pattern formation facilitates the avoidance of this undesired conversion and the subsequent observation of the mechanical action of the 'pure' spin flow without any contamination influence of the orbital one.

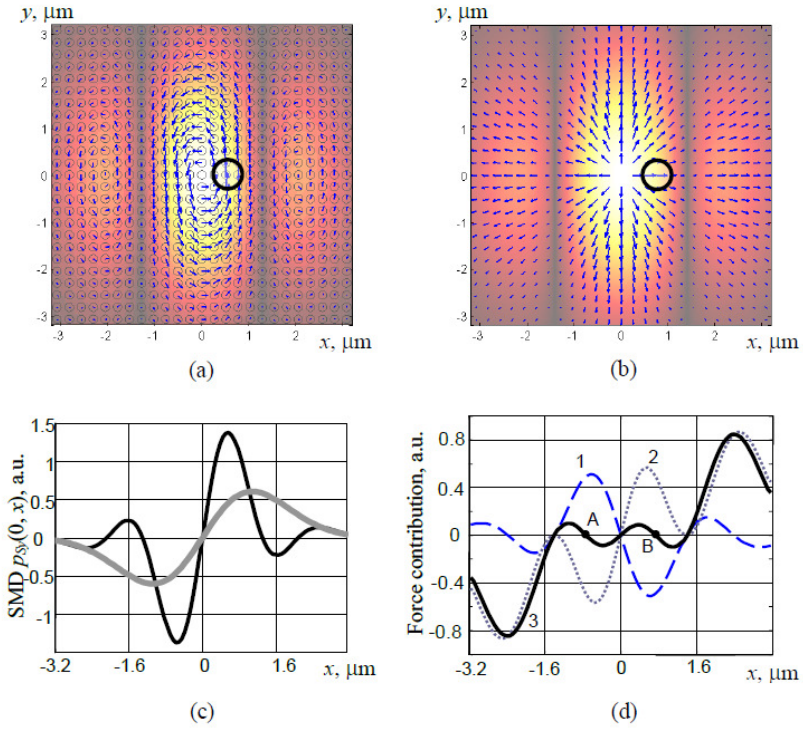

Fig. 2. Characteristics of the optical field in the observation plane (see Fig. 1) for $\sigma = 1$, viewed against the z-axis. (a) SMD and (b) OMD maps (arrows) with the intensity distribution as a background; (c) actual SMD distribution along the x-axis (black curve) together with the SMD distribution for a single focused Gaussian beam with the same sum power (light curve); (d) qualitative pattern of the transverse forces experienced by a probe particle at the x-axis: gradient force (curve 1), OMD-generated radial light pressure force (curve 2) and resulting force (black curve), A and B are points of stable equilibrium. In panel (a), polarization ellipses are shown on the background (because of small θ, they have small eccentricities and visually look like circles); panels (a) and (b) also contain contours of a trapped particle (black circle) located at point B of panel (d).

#159576 - $15.00 USD Received 7 Dec 2011; revised 23 Jan 2012; accepted 23 Jan 2012; published 30 Jan 2012

4. Results and discussion

In the experiment, a cell was used that contained an ensemble of latex microparticles (refractive index 1.48) suspended in water. The particles were chosen so that their shape was close to ellipsoidal with approximate size 1.5 × 1 μm, which was suitable for observing individual particles within a single lobe of the interference pattern formed in the focal region.

Experimental observations of the trapped particle motion in case when both superposed beams were circularly polarized are represented by the video in Fig. 3. It is seen that the asymmetric particle spins around its own centre of mass, which is naturally explained by partial absorption of the incident circularly polarized light together with its inherent angular momentum. This effect is well known [24,27] and to be expected in this situation. A new observation is that, simultaneously, the particle's centre of mass evidently performs an orbital motion, which can only be associated with the azimuthal light pressure originating from the SMD circulation (see Fig. 2a). This attribution is confirmed by the reversal of rotational direction when the sign of the circular polarization is changed; besides, when both beams are linearly polarized, the particle stops.

Hence, the preliminary suggestion that the spin energy flow of an inhomogeneous circularly polarized beam can cause translational and orbital motion of probe particles is experimentally verified. Among other things, this means that the usual believe that orbital motion of particles witnesses for the orbital angular momentum in the motive light field is generally not correct, and possible contribution of the spin flow must be taken into account in experiments on the spin-to-orbital angular momentum conversion [26,30]. In fact, in the known work treating this issue, in particular, Ref [26], the spin flow action is absent or negligible, and their conclusions are correct.

Fig. 3. Motion of a particle trapped within the central lobe of the interference pattern of Fig. 2. Media 1.

It should be emphasized that beams with inhomogeneous intensity distribution and uniform circular polarization, as employed in this paper, are not unique examples of light field with nonzero SMD. In accordance with Eqs. (6), (7), quite similar SMD should appear in polarization-inhomogeneous beams. Such situations were recently discussed [36] but wrongly interpreted [37] as manifestations of a new category of the orbital angular momentum. Besides, high-NA focusing reported in Ref [36]. gives no certainty that the observed orbital motion of trapped particles is not caused by the OMD generated due to the spin-to-orbital conversion.

#159576 - $15.00 USD Received 7 Dec 2011; revised 23 Jan 2012; accepted 23 Jan 2012; published 30 Jan 2012

5. Conclusions

To the best of our knowledge, the results reported in this paper can be considered as the first experimental evidence for the mechanical action of the spin momentum of light fields. This purports an additional confirmation for the mechanical equivalence of the spin and orbital momentum of light, despite the difference in their physical nature [12,16]. Additionally, we have demonstrated possibility of the SMD-induced particle transportation, which probably constitutes an interesting applied aspect of the observed phenomena. In our opinion, such a possibility opens up new promising opportunities for controllable optical manipulation procedures in which regulation and regime switching are realized via the polarization control alone, without change of the trapping beam intensity or spatial profile. Such techniques may be advantageous in many applications, e.g., when high switching speed is important.

#159576 - $15.00 USD Received 7 Dec 2011; revised 23 Jan 2012; accepted 23 Jan 2012; published 30 Jan 2012